Hitting and trapping times on branched structures

Elena Agliari,[1,2] Fabio Sartori,[3,*] Luca Cattivelli,[4] and Davide Cassi[3]

[1]*Dipartimento di Fisica, Sapienza Università di Roma, 00185 Roma, Italy*
[2]*Università Campus Bio-Medico, Roma, Italy*
[3]*Dipartimento di Fisica e Scienze della Terra, Università di Parma, Parma, Italy*
[4]*Scuola Normale Superiore, Pisa, Italy*

In this work we consider a simple random walk embedded in a generic branched structure and we find a close-form formula to calculate the hitting time $H(i,f)$ between two arbitrary nodes i and j. We then use this formula to obtain the set of hitting times $\{H(i,f)\}$ for combs and their expectation values, namely, the mean first-passage time, where the average is performed over the initial node while the final node f is given, and the global mean first-passage time, where the average is performed over both the initial and the final node. Finally, we discuss applications in the context of reaction-diffusion problems.

I. INTRODUCTION

Random walks (RWs) on inhomogeneous structures were first introduced to describe anomalous diffusion [1–3], but they actually constitute a convenient model for many real phenomena, ranging from soft matter (e.g., gels and biological structures [4]) to condensed matter (e.g., fractures [5] and light scattering [6]). Here, we focus on the so-called "branched structures," namely, graphs $\mathcal{V}$ obtained by attaching to each vertex j of a base graph $\mathcal{G}_0$ a different graph $\mathcal{G}_j$ called the fiber (see Fig. 1). In particular, we consider a specific class of branched structures called combs, namely, graphs where the base graph as well as the fiber ones are linear chains, in such a way that $\mathcal{G}_j$ is site independent and equivalent to $\mathbb{Z}$ (see Fig. 2). Combs and diffusion on combs are extensively used to mimic a number of systems, e.g., branched polymers [7,8], transport of calcium in spiny dendrites [9,10], excitation of nanoantennas [11], anomalous diffusion in percolation structures [12–16], cancer proliferation [17], diffusion of particles in crowded environments [2,18], diffusion of ultracold atoms [19], and chromatography or hydrodynamic dispersion [20], and also to produce quantum devices, such as arrays of Josephson junctions, microbridges, or quantum wires [21].

Diffusion on combs has been shown to display many peculiar features, ultimately stemming from their highly inhomogeneous topology (see, e.g., [22–26]). Now, most of the previous results have been proven in the thermodynamic limit, namely, for structures of infinite size, while real systems are intrinsically finite. In this work we aim to investigate the problem of diffusion in finite comb lattices and we especially focus on first-passage quantities such as the hitting time $H(i,f)$ from i to f (i.e., the mean time for a random walker first to reach site f, starting from i), the mean first-passage time to f (MFPT$_f$) (i.e., the mean time needed first to reach the vertex f, averaged over the starting site), and the global mean first-passage time GMFPT (i.e., the mean time to go from a random vertex to a second random vertex).

These quantities are fundamental in the study of transport limited reactions, because they provide the characteristic reaction time in the limit of a perfect reaction. In particular, these quantities have been extensively studied in the past, in relation to different applications in several research areas: pharmacokinetics [27], reaction-diffusion processes [28], excitation transport in photosystems [29,30], target search processes [31], spread of disease [32], and many other physical problems [33–39]. Pharmacokinetics and reaction-diffusion processes could also be affected by the occupation time, namely, the mean time spent in a subset of the graph's vertices [40,41].

In general, mean-first-passage-related observables (e.g., MFPT, splitting probabilities, occupation time distributions) permit a quantitative analysis of the kinetics of transport-limited reactions. Moreover, such first-passage observables have recently been shown to provide tools to unambiguously discriminate among possible microscopic scenarios of sub-diffusion (e.g., stemming from waiting times in the particle dynamics or from the peculiar underlying topology) [42].

In this work we calculate the MFPT and the GMFPT for (d-dimensional) combs using the resistance method: the original graph $\mathcal{V}$ is mapped into a resistance network by replacing any link (a,b) between two adjacent nodes a and b with a unitary resistance R [43]. Then we use Tetali's formula [44] to calculate the exact value of the hitting time between i and f as

$$H(i,f) = mR_{i,f} + \frac{1}{2}\sum_{z \in V} g(z)\{R_{f,z} - R_{i,z}\}, \qquad (1)$$

where m is the number of links in the graph, $g(z)$ is the coordination number of the vertex z, and $R_{a,b}$ is the effective resistance between vertex a and vertex b.

II. HITTING TIME OF BRANCHED STRUCTURES

In this section we use Eq. (1) to calculate the value of the hitting time for generic branched structures (see Fig. 1). When the starting point i and the ending point f belong to different fibers, we can divide the vertices of $\mathcal{V}$ into three disjoint subsets, referred to as $\mathcal{I}$, $\mathcal{F}$, and $\mathcal{B}$, respectively (see Fig. 3): $\mathcal{V} = \mathcal{I} \cup \mathcal{F} \cup \mathcal{B}$. More precisely, subset $\mathcal{I}$ contains all vertices belonging to the fiber graph $\mathcal{G}_i$, subset $\mathcal{F}$ contains all vertices
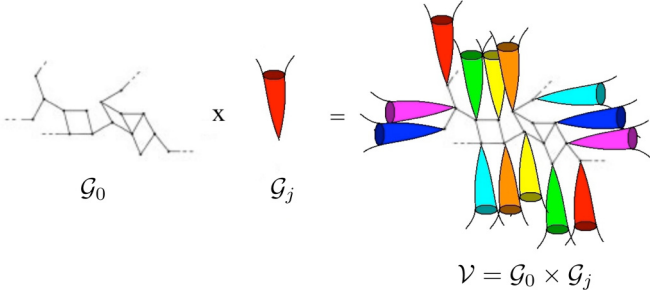
*fabio.sartori@studenti.unipr.it

FIG. 1. (Color online) Example of the branched structure $\mathcal{V}$ obtained by joining to each point j of a graph $\mathcal{G}_0$, called the base (left), a graph $\mathcal{G}_j$, called the fiber (middle).

belonging to the fiber graph $\mathcal{G}_f$, and, finally, subset $\mathcal{B}$ contains all vertices belonging to the fiber graphs $\mathcal{G}_k$ corresponding to the set of sites $\mathcal{K}_k$, with $k \neq (i,f)$, and $\mathcal{B} = \bigcup_{k \neq i,f} \mathcal{K}_k$.

This procedure allows us to write the sum in (1) as

$$\sum_{z \in \mathcal{V}} g(z)(R_{f,z} - R_{i,z}) = \sum_{z \in \mathcal{I}} g(z)(R_{f,z} - R_{i,z})$$
$$+ \sum_{z \in \mathcal{F}} g(z)(R_{f,z} - R_{i,z})$$
$$+ \sum_{z \in \mathcal{B}} g(z)(R_{f,z} - R_{i,z}); \quad (2)$$

namely, we distinguish the case where z is in the same fiber graph as i ($z \in \mathcal{I}$), z is in the same fiber graph as f ($z \in \mathcal{F}$), and z is in a fiber graph which neither i nor f belongs to ($z \in \mathcal{B}$). In the following we call root r_i the vertex shared by the base graph $\mathcal{G}_0$ and the fiber graph $\mathcal{G}_i$.

In general, when two vertices, i and f, belong to different fiber graphs, we can write the effective resistance $R_{i,f}$ between
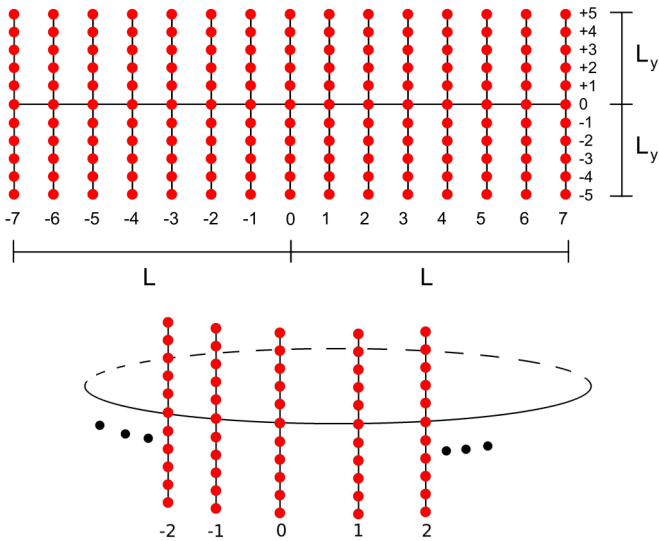

FIG. 2. (Color online) Examples of two-dimensional combs, where the backbone is endowed with reflecting boundary conditions (top) or periodic boundary conditions (bottom). The size of the backbone is referred to as $2L + 1$, while the length of the teeth L_y is taken to be uniform and to scale linearly with L, namely, $L_y = \alpha L$. For instance, at the top $L = 7$ and $\alpha L = 5$.
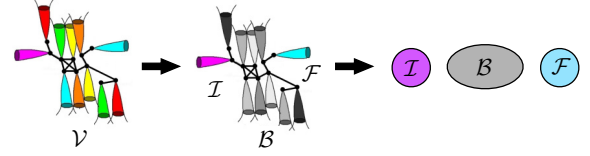

FIG. 3. (Color online) Schematization of the decomposition used in Eq. (2), where $\mathcal{V} = \mathcal{I} \cup \mathcal{F} \cup \mathcal{B}$. Note that the whole set of fiber graphs $\{\mathcal{G}_k\}$ also includes the set of nodes making up the base graph because the joining nodes, also called "roots," are shared.

these points as the sum of three resistances in series:

$$R_{i,f} = R_{i,r_i} + R_{r_i,r_f} + R_{f,r_f}. \quad (3)$$

Now, recalling Eq. (2), we can note that when $z \in \mathcal{B}$ we can use Eq. (3) for both $R_{i,z}$ and $R_{z,f}$, while when $z \in \mathcal{I}$ or $z \in \mathcal{F}$, we can use Eq. (3) only for $R_{i,z}$ or for $R_{i,z}$, respectively. In fact, suppose we consider a linear chain as a fiber graph $\mathcal{G}_i$: when z and i belong to the same fiber graph the effective resistance according to Eq. (3) would be $|y_i| + |y_z|$, y_i and y_f being the coordinates of i and f along the related teeth, while the correct estimate is $|y_i - y_f|$, which recovers the former only when the signs are different.

Exploiting this remark, the three sums appearing in Eq. (2) can be written as

$$\sum_{z \in B} g(z)(R_{f,z} - R_{i,z}) = \sum_{z \in B} g(z)\{R_{r_f,r_z} - R_{r_i,r_z}$$
$$+ R_{f,r_f} - R_{i,r_i}\},$$

$$\sum_{z \in I} g(z)(R_{f,z} - R_{i,z}) = \sum_{z \in I} g(z)\{R_{f,r_f} + R_{r_f,r_z}$$
$$+ R_{z,r_z} - R_{i,z}\},$$

$$\sum_{z \in F} g(z)(R_{f,z} - R_{i,z}) = \sum_{z \in F} g(z)\{R_{f,z} - R_{i,r_i}$$
$$- R_{r_i,r_z} - R_{z,r_z}\}.$$

Then, after some algebraic manipulations we find

$$H(i,f) = m R_{r_i,r_f} + \frac{1}{2}\sum_{z \in \mathcal{V}} g(z)(R_{r_f,r_z} - R_{r_i,r_z})$$
$$+ 2(m - m_f)R_{f,r_f} + H_i(i,r_i) + H_f(r_f,f), \quad (4)$$

where m_k is the number of links in subgraph $\mathcal{G}_k$, and $H_k(a,b)$ is the mean time for a walker to go from a to b, $(a,b \in \mathcal{G}_k)$, without ever coming out from fiber $\mathcal{G}_k$.

The previous equation, (4), is similar to that with which we began, (1), but now resistances are considered between points of the base graph. This allows us to factorize the difference $(R_{r_f,r_z} - R_{r_i,r_z})$, by splitting the summation over $z \in \mathcal{V}$ into the summation over every vertex of the base graph and of all fiber graphs:

$$\sum_{z \in \mathcal{V}} g(z)(R_{r_f,r_z} - R_{r_i,r_z}) = \sum_{k \in \mathcal{G}_0} \sum_{z \in \mathcal{G}_k} g(z)(R_{r_f,r_z} - R_{r_i,r_z})$$
$$= \sum_{z \in \mathcal{G}_k} g(z) \sum_{k \in \mathcal{G}_0} (R_{r_f,r_k} - R_{r_i,r_k})$$
$$= \sum_{k \in \mathcal{G}_0} (R_{r_f,r_k} - R_{r_i,r_k}) 2m_k. \quad (5)$$

Finally, merging Eqs. (4) and (5), we get

$$H(i,f) = H_i(i,r_i) + \sum_{k \in \mathcal{G}_0} m_k \left(R_{r_f,r_k} - R_{r_k,r_i} \right)$$
$$+ m R_{r_i,r_f} + H_f(r_f,f) + 2(m - m_f) R_{f,r_f}. \quad (6)$$

Of course, this formula recovers the Tetali one, (1), when all the branched graphs $\mathcal{G}_k$ are composed of only a single vertex (the one that is shared with $\mathcal{G}_0$, i.e., the root r_k). The details of the fibers only enter in the summation term, and in particular, only their position and the number of their links m_k matter, while neither the topology nor the number of vertices of these fiber graphs affects $H(i,f)$.

A. Particular cases

There are special cases where the formula in Eq. (6) can be significantly simplified. For instance, when the ratio between the coordination number $g(r_k)$ of any root r_k belonging to the base graph and the number of links m_k in the kth subgraph is independent of k. This allows us to write $m_k = \gamma g(r_k)$, γ being a constant value which is the same for every vertex of the base graph $\mathcal{G}_0$. Then the summation in Eq. (6) becomes

$$\sum_{k \in \mathcal{G}_0} m_k \left(R_{r_f,r_z} - R_{r_i,r_z} \right) = 2\gamma [H_0(r_i,r_f) - m_0 R_{r_f,r_i}], \quad (7)$$

and using this result, Eq. (6) becomes

$$H(i,f) = H_i(i,r_i) + 2\gamma H_0(r_i,r_f) + H_f(r_f,f)$$
$$+ 2(m - m_f) R_{f,r_f} + (m - 2\gamma m_0) R_{r_i,r_f}, \quad (8)$$

where $H_i(a,b)$ and $H_f(a,b)$ represent the mean time taken by a walker first to go from a node a to a node b (with $a,b \in \mathcal{I}$ and $a,b \in \mathcal{F}$ respectively) without ever leaving $\mathcal{I}$ and $\mathcal{F}$, respectively; analogously, $H_0(a,b)$ represents the mean time first to reach b, starting from a (with $a,b \in \mathcal{G}_0$) and moving only on the base graph. In this case the mean time to go from i to f can be expressed by the sum of three hitting times and a constant term.

Another interesting case appears when the position of the root of the starting vertex r_i and the root of the ending one r_f displays a symmetry such that

$$H(r_i,r_f) = H(r_f,r_i). \quad (9)$$

In this case, Eq. (6) becomes

$$H(i,f) = H_i(i,r_i) + H_f(r_f,f)$$
$$+ 2(m - m_f) R_{f,r_f} + m R_{r_i,r_f}. \quad (10)$$

This formula allows us to calculate the hitting times for any "symmetric structure" [according to Eq. (9)], like a Sierpinski gasket branched with linear chains (see Fig. 4).

Let us consider a Sierpinski gasket of generation n and, as fibers, linear chains with L vertices. The total number of vertices in the base graph is $|V|_0^{(n)} = 3(3^n + 1)/2$ and the total number of links is $m_0^{(n)} = 3^{n+1}$ [45]. For instance, let us try to evaluate the mean time first to reach the node f belonging to a tooth stemming from a corner, starting from a node i belonging to a tooth stemming from another corner (see Fig. 4). As shown in [46], $R_{r_i,r_f} = 2 \cdot 5^n / 3^{n+1}$, while, recalling results
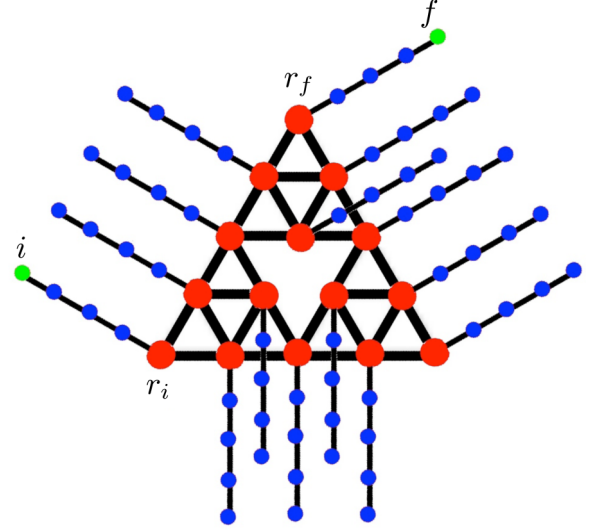

FIG. 4. (Color online) Example of a Sierpinski gasket of generation $n = 3$, branched with linear chains with $L = 5$ vertices.

valid for linear chains, $H(i,f) = 2L|i - f| + f^2 - i^2$, with $i,f = -L, \ldots, +L$ [37]. Inserting these partial results into Eq. (10), we get that, for the above-mentioned choice of i and f, the mean time reads as

$$H(i,f) = 3L^2 + \left(1 + \frac{L}{2}\right)(3^{n+1} + 2 \cdot 5^n) + \left(\frac{5}{3}\right)^n L.$$

B. Bidimensional combs

Bidimensional combs are branched structures where the base graph $\mathcal{G}_0$ is a *one*-dimensional lattice, like a linear chain or a ring, usually called the *backbone*, and fiber graphs are linear chains usually called *teeth* (see Fig. 2.) Here, we consider two cases according to the boundary conditions applied to the backbone: we call combs whose backbone is a linear chain "bidimensional open combs" and combs whose backbone is a ring "bidimensional closed combs"; teeth are always taken as open (i.e., reflecting at boundaries). As shown in Fig. 2, the size of the backbone is $2L + 1$, and each linear chain departing from the backbone counts αL vertices, in such a way that α measures the relative geometrical importance of the side branches (e.g., when $\alpha = 1$ the comb is square).

Using Eq. (6) we are now able to calculate the value of $H(i,f)$ for these graphs. In the following, exploiting the fact that combs are embedded in two-dimensional lattices, the position of the arbitrary point k is denoted $\{x_k, y_k\}$ where x_k indicates the projection of k on the backbone, and y_k its height along the related tooth.

Let us start with open combs, where the resistance between two generic points $a = (x_a, y_a)$ and $b = (x_b, y_b)$ can be written as

$$R_{a,b} = \delta_{x_a,x_b} |y_a - y_b|$$
$$+ \left(1 - \delta_{x_a,x_b}\right)(|x_a - x_b| + |y_a| + |y_b|). \quad (11)$$

Thus, with some algebra, Eq. (6) can be restated as[1]

$$H(i,f) = mR_{i,f} + \left(y_f^2 - y_i^2\right) + (2\alpha L + 1)\left(x_f^2 - x_i^2\right)$$
$$+ \left(|y_2| - |y_1|\right)\left(L^2 4\alpha + 2L\right). \qquad (12)$$

From this equation we can extract important information, such as the mean time to cross the whole backbone and the mean time to "climb" a tooth. These quantities are, respectively,

$$H\left(-L, 0 \to L, 0\right) = L^3(8\alpha) + L^2(4 + 4\alpha)$$

and

$$H\left(\{0,0\} \to \{0, \alpha L\}\right) = L^3(8\alpha^2) + L^2(4\alpha + 3\alpha^2).$$

Let us now consider closed combs (whose related quantities are denoted by the symbol ↻), for which the resistance between two generic points $a = (x_a, y_a)$ and $b = (x_b, y_b)$ is

$$R_{a,b}^{\circlearrowright} = \delta_{x_a, x_b}|y_a - y_b| + (1 - \delta_{x_a, x_b})$$
$$\times \left(|x_a - x_b| + |y_a| + |y_b| - \frac{(x_a - x_b)^2}{2L + 1}\right),$$

and the hitting time $H^{\circlearrowright}(i,f)$ from i to f follows from Eq. (6) as[2]

$$H_2^{\circlearrowright}(i,f) = mR_{if}^{\circlearrowright} + (|y_f| - |y_i|)[4\alpha L^2 + 2L + 1]$$
$$+ \left(y_f^2 - y_i^2\right). \qquad (13)$$

From Eq. (13) we can extract the time needed to cross half the backbone as

$$H_2^{\circlearrowright}(\{0,0\} \to \{L,0\}) = L^3(6\alpha) + L^2(3 + 2\alpha) + L,$$

and the time to climb a tooth as

$$H_2^{\circlearrowright}(\{0,0\} \to \{0, \alpha L\}) = L^3(8\alpha^2) + L^2(4\alpha + 3\alpha^2) + L(2\alpha).$$

We note that the leading order of the mean time needed to cross the backbone is proportional to α (consistent with results in [37]) and the leading order of the mean time to climb a tooth is proportional to α^2.

C. *d*-dimensional open combs

We define *d*-dimensional open combs recursively (see also Fig. 5):

(a) a one-dimensional open comb is a linear chain;

(b) a two-dimensional open comb is a branched graph $\mathcal{G}$, whose base graph is a linear chain and whose fiber graphs are linear chains;

(c) ...;

---

[1]What we really find from Eq. (6) is $(i,f) - 2L(1 + \alpha + 2\alpha L)[-1 + |y_i| + |y_f| - |y_i - y_f|]\delta_{x_i,x_f}$. This difference is due to the hypothesis that $x_i \neq x_f$; namely, the starting point and the final point belong to different fiber graphs. If we use Eq. (8) instead of Eq. (6), we introduce an additional error of $(x_i - x_f)(x_i + x_f)$ due to the different value of $g(x,0)$ between $x = \pm L$, where $g(\pm L, 0) = 3$, and $x \neq \pm L$, where $g(x,0) = 4$.

[2]Once again, what we really find using Eq. (6) is $H_2^{\circlearrowright}(i,f) - (1 + 2L)(1 + 2\alpha L)[|y_i| + |y_f| - |y_i - y_f|]\delta_{x_i,x_f}$. This difference is due to the hypothesis that $x_i \neq x_f$. This time if we use Eq. (8) instead of Eq. (6), we do not introduce any additional error.
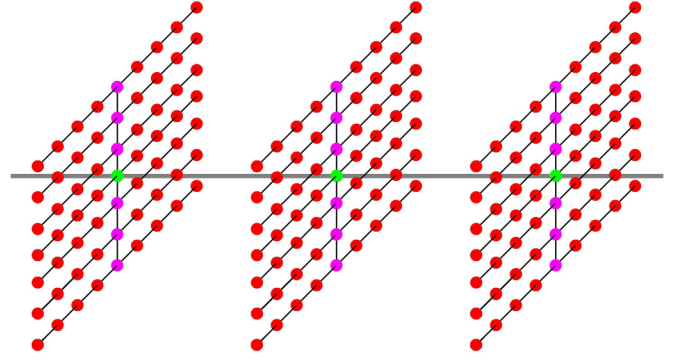

FIG. 5. (Color online) Example of a three-dimensional comb. Vertices which belong to the first generation are shown in green; those which belong to the second, in lilac; and those which belong to the third, in red.

(d) a *d*-dimensional open comb is a branched graph $\mathcal{G}$ whose base graph is a $(d-1)$-dimensional comb and whose fibers are linear chains.

As shown in Sec. II B, a finite two-dimensional comb can be defined by fixing two parameters: the length of the backbone L and the ratio α between the length of a tooth and the length of the backbone, in such a way that the thermodynamic limit $L \to \infty$ is well defined. Now, to fix a *d*-dimensional comb we introduce *d* parameters: $(L, \alpha_2, \ldots, \alpha_d)$, α_i being the ratio between the length of the tooth in the *i*th direction (i.e., added at the *i*th iteration) and the length of the backbone, $\alpha_i = L_i/L$.

We label every vertex with *d* coordinates and call $i = (x_1, \ldots, x_d)$ and $f = (y_1, \ldots, y_d)$, where the first coordinate labels the vertices on the base graph and it takes a value from $-L$ to L, the second one goes from $-\alpha_2 L$ to $\alpha_2 L$ and labels the vertices of the fiber graphs, the third one goes from $-\alpha_3 L$ to $\alpha_3 L$, and so on.

We define $H^{(d)}(i,f)$, the hitting time from i to f in a *d*-dimensional comb. Using Tetali's equation we can see that $H^{(d)}(i,f) \sim \mathcal{O}(L^{d+1})$. In fact, the first term on the right-hand side in Eq. (1) is $m_d R_{i,f}$, and one can see that in the *d*-dimensional comb the number of links m_d is

$$m_d \sim \left(L^d 2^d \prod_{k=2}^{d} \alpha_k\right), \qquad (14)$$

while the maximum value of R is

$$R = 2L\left(1 + \sum_{k=2}^{d} \alpha_k\right) + 1;$$

thus, the leading order of this first term is L^{d+1}. Also, the second term on the right-hand side of Eq. (1), that is, $\frac{1}{2}\sum_{z \in \mathcal{V}} g(z)(R_{f,k} - R_{k,i})$, where $g(z) \leqslant 2d = \mathcal{O}(L^0)$, $|\mathcal{V}| = \mathcal{O}(L^d)$, and $R = \mathcal{O}(L)$, is order L^{d+1}. Now, using these remarks, we can handle Eq. (6) to get a finer estimate for the asymptotic expression of $H^{(d)}(i,f)$. The leading order of Eq. (6) is given by

$$H(i,f) \sim \frac{1}{2}\sum_{k=0}^{L}\{|k - y_1| - |k - x_1|\}m_k$$
$$+ 2m_d R(f, r_f) + m_d R_{r_i, r_f}. \qquad (15)$$

We have just pointed out that $m_d \sim (L^d 2^{d-1} \prod_{k=2}^d \alpha_k)$, where m_k is the number of links in the fiber graph starting from node k, and its leading value is $m_k \sim (L^{d-1} 2^{d-1} \prod_{k=2}^d \alpha_k)$; thus

$$H(i,f)^{(d)} \sim \left(L^{d-1} 2^{d-2} \prod_{k=2}^d \alpha_k \right) \left(y_1^2 - x_1^2 \right)$$
$$+ \left(L^d 2^d \prod_{k=2}^d \alpha_k \right) \left[|x_1 - y_1| + 2\sum_{j=2}^d |y_j| \right].$$

By introducing the normalized coordinates $\xi_i = y_i/(\alpha_i L)$ and $\eta_i = x_i/(\alpha_i L)$ (posing conventionally $\alpha_1 = 1$), we can express the leading value of $H^{(d)}(i,f)$:

$$H(\vec{\eta}, \vec{\xi}) \sim L^{d+1} 2^{d-2} \prod_{i=2}^d \alpha_i$$
$$\times \left[(\xi_1^2 - \eta_1^2) + 4|\xi_1 - \eta_1| + 8\sum_{k=2}^d \alpha_k \xi_k \right]. \tag{16}$$

We can use Eq. (16) to calculate the mean time to cross the backbone going from $\eta = (-1, \vec{0})$ to $\xi = (+1, \vec{0})$ as

$$H^{(d)}(\{-1,\vec{0}\} \to \{1,\vec{0}\}) \sim L^{d+1} 2^{d+1} \prod_{i=2}^d \alpha_i$$

and its maximum value going from $\eta = (-1, \vec{1})$ to $\xi = (1, \vec{1})$ as

$$H^{(d)}(\{-1,\vec{1}\} \to \{+1,\vec{1}\}) \sim L^{d+1} 2^{d+1} \prod_{i=2}^d \alpha_i \left[1 + \sum_{k=2}^d \alpha_k \right].$$

For instance, for a square d-dimensional comb (i.e., $\alpha_i = 1, \forall i$) we get $H^{(d)}(\{-1,\vec{0}\} \to \{1,\vec{0}\}) \sim 2^{d+1} L^{d+1}$ and $H^{(d)}(\{-1,\vec{1}\} \to \{+1,\vec{1}\}) \sim 2^{d+1} d L^{d+1}$.

III. TRAPPING TIMES

In this section, we analyze the MFPT, defined by $\mathrm{MFPT}_f = \mathbb{E}_i[H(i,f)]$ and the GMFPT, defined by $\mathrm{GMFPT} = \mathbb{E}_i[\mathbb{E}_f[H(i,f)]]$. The former represents the mean time to reach a fixed reaction node placed in f, starting from a random one. The latter is the mean time to reach a random vertex starting from another random one.

A. MFPT$_f$

The MFPT$_f$ was introduced by Montroll for regular graphs [29] to describe the excitation transfer on a photosintetic complex. Later this quantity was extended to irregular graphs (see [22,33,37,47–49]). Once we know every value of $H(i,f)$ we can calculate this quantity exactly using $\mathrm{MFPT}_f = V^{-1} \sum_{i \in \mathcal{V}} H(i,f)$, where V is the volume of the graph $\mathcal{V}$.

1. Bidimensional open combs

Equation (12) provides the values of $H(i,f)$ for every couple of nodes (i,f), and in order to get MFPT$_f$, it is convenient to split Eq. (12) into three parts,

$$H(i,f) = \{mR_{if}\} + \left\{ (2\alpha L + 1)\left(x_f^2 - x_i^2 \right) \right\}$$
$$+ \left\{ (y_f^2 - y_i^2) + (|y_f| - |y_i|)(L^2 4\alpha + 2L) \right\}$$
$$= A + B + C,$$

and average these contributions over i separately. The first contribution, $\mathbb{E}_i[A]$, can be written as

$$\mathbb{E}_i[A] = \sum_{x_i=-L}^{L} \sum_{y_i=-\alpha L}^{L} m \left[\delta_{x_i,xf} |y_i - y_f| \right.$$
$$\left. + \left(1 - \delta_{x_i,xf} \right)(|x_i - x_f| + |y_i| + |y_f|) \right],$$

and after the summation on x_i it becomes

$$\mathbb{E}_i[A] = \frac{m}{V} \sum_{y_i=-\alpha L}^{\alpha L} \left\{ |y_i - y_f| \right.$$
$$\left. + 2L \left(|y_i| + |y_f| + x_f^2 + L + L^2 \right) \right\}$$

and, finally,

$$\mathbb{E}_i[A] = y_f^2 \frac{m}{V} + |y_f| \left[\frac{m}{V} (2\alpha L + 1) 2L \right]$$
$$+ x_f^2 \left[\frac{m}{V} (2\alpha L + 1) \right] + \frac{m}{V} [\alpha L (\alpha L + 1)$$
$$+ L(L+1)(2\alpha L + 1) + 2\alpha L^2 (\alpha L + 1)].$$

Performing similar calculations for the second and third contributions, we get, respectively,

$$\mathbb{E}_i[B] = \sum_{x_i,y_i} \left[(2\alpha L + 1)\left(x_f^2 - x_i^2 \right) \right]$$
$$= (2\alpha L + 1) x_f^2 - \frac{1}{3} L(L+1)(2\alpha L + 1),$$

$$\mathbb{E}_i[C] = |y_f| 2L(2\alpha L + 1) - y_f^2 - \alpha L \left(\frac{1}{3} + 2L \right).$$

Merging these three contributions we find the exact value of MFPT$_f$:

$$\mathrm{MFPT}_{\{x_f,y_f\}}$$
$$= \left(1 + \frac{m}{V} \right) \left[y_f^2 + x_f^2 (2\alpha L + 1) |y_f| (4\alpha L^2 + 2L) \right]$$
$$+ \frac{1}{3(1 + 2L)(1 + 2\alpha L)}$$
$$\times [16\alpha^2 L^5 + L^4(16\alpha + 24\alpha^2 + 8\alpha^3) - L(1 + \alpha)$$
$$+ L^2 3(1 + \alpha) + L^3(4 + 18\alpha + 14\alpha^2 + 4\alpha^3)]. \tag{17}$$

The position of the trap affects only the contribution in the first square bracket. Therefore, $\mathrm{MFPT}_{(x_f,y_f)}$ can be written as the sum of two terms: the former depends on the final vertex, and the latter depends only on L and α and is exactly MFPT$_{\{0,0\}}$ (i.e., the mean time first to reach the central node),

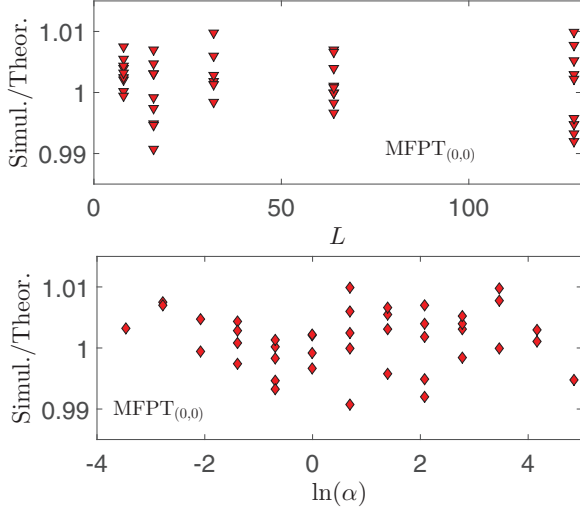$$\mathrm{MFPT}_{\{x_f,y_f\}}(L,\alpha) = \phi(x_f, y_f) + \mathrm{MFPT}_{\{0,0\}}, \tag{18}$$

FIG. 6. (Color online) Numerical check of the theoretical predictions of Eq. (17) for $\{x_f, y_f\} = \{0,0\}$. In both panels the results of the simulations are divided by the theoretical value of MFPT$_{\{0,0\}}$.

where

$$\phi(x_f, y_f) = \left(1 + \frac{m}{V}\right)\left[y_f^2 + x_f^2\left(2\alpha L + 1\right)\right.$$
$$\left. \times |y_f|(4\alpha L^2 + 2L)\right]. \quad (19)$$

We have numerically tested this result for three positions of the trap (x_f, y_f) and for several values of L and α, as shown in Figs. 6, 7, and 8. In each of these figures the value of (x_f, y_f) is fixed and we change the value of L and α. The values of (x_f, y_f) are, respectively, $(0,0)$, $(L,0)$, and $(L,\alpha L)$; L takes values from 8 to 256; and α goes from $1/32$ to 128.

The asymptotic behavior of MFPT$_f$ is

$$\text{MFPT}_f(L,\alpha) \sim L^3 \left\{ 4\alpha\left[\frac{1}{3} + \left(\frac{x_f}{L}\right)^2\right] + 8\alpha\left|\frac{y_f}{L}\right|\right\}$$
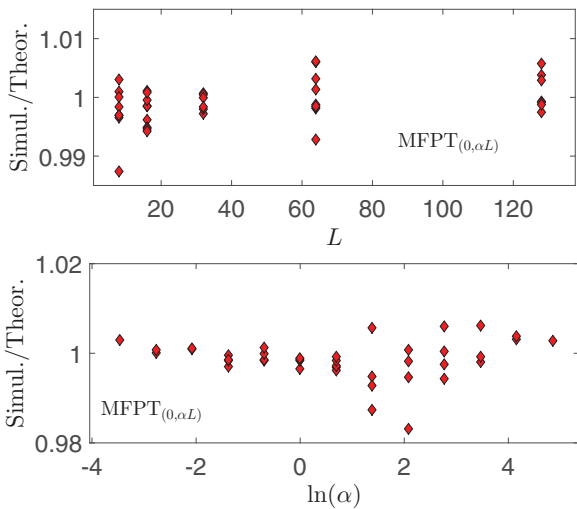$$\sim \frac{4}{3}\alpha L^3, \quad (20)$$

FIG. 7. (Color online) Numerical check of the theoretical predictions of Eq. (17) for $\{x_f, y_f\} = \{0,\alpha L\}$. In both panels the results of the simulations are divided by the theoretical value of MFPT$_{\{0,\alpha L\}}$.
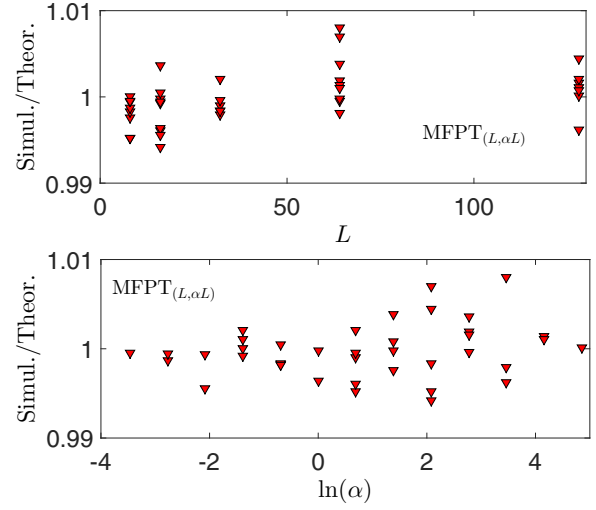

FIG. 8. (Color online) Numerical check of the theoretical predictions of Eq. (17) for $\{x_f, y_f\} = \{L,\alpha L\}$. In both panels the results of the simulations are divided by the theoretical value of MFPT$_{\{L,\alpha L\}}$.

where the latter relation holds as long as both x_f and y_f are finite. The dependence on L^3 is consistent with previous asymptotic results [26,37].

2. Bidimensional closed combs

Analogous arguments can be applied to calculate the exact value of the MFPT for closed combs, and we call this quantity the MFPT$_f^{\circlearrowleft}$. We skip lengthy passages (analogous to those described above for the open comb) and provide straightforwardly the final result:

$$\text{MFPT}_{(x_f, y_f)}^{\circlearrowleft} = |y_f|(1 + 4L + 8L^2\alpha) + 2y_f^2 + \frac{1}{3 + 6\alpha L}$$
$$\times [L(2 - \alpha) + L^2(2 + 8\alpha + 3\alpha^2)$$
$$+ L^3 4\alpha(2 + 2\alpha + \alpha^2) + L^4(8\alpha^2)]. \quad (21)$$

Of course, MFPT$_f^{\circlearrowleft}$ does not depend on x_f, due to the periodic condition on the x axis. Moreover, as done in Eq. (18) we can distinguish two contributions highlighting the dependence of the trap position (i.e., the height y_f) as

$$\text{MFPT}_{(x_f, y_f)}^{\circlearrowleft}(L,\alpha) = \phi^{\circlearrowleft}(y_f) + \text{MFPT}_{(0)},$$

where

$$\phi^{\circlearrowleft}(y_f) = |y_f|(1 + 4L + 8L^2\alpha) + 2y_f^2. \quad (22)$$

The asymptotic behavior reads as

$$\text{MFPT}_f^{\circlearrowleft}(L,\alpha) \sim L^3\left\{\frac{4}{3}\alpha + 8\alpha\frac{y_f}{L}\right\} \sim \frac{4}{3}\alpha L^3, \quad (23)$$

where the last relation holds as long as y_f is finite.

We have numerically tested this result for two values of y_f and for several values of L and α, as shown in Figs. 9 and 10. In each of these figures the value of y_f is fixed and we change the value of L and α. The values of y_f are, respectively, 0 and αL; L takes values from 8 to 256; and α goes from $1/32$ to 128.
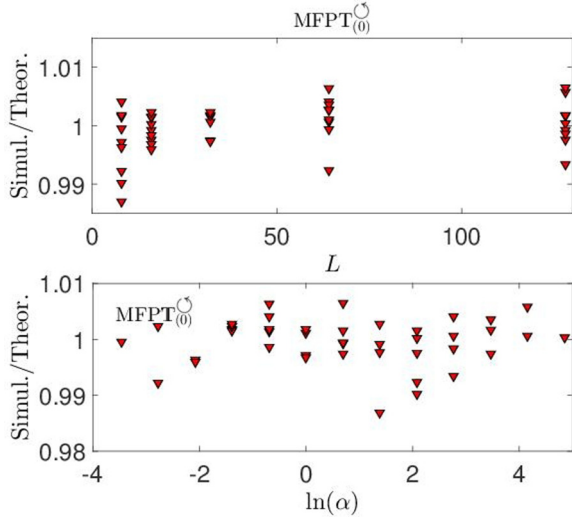
FIG. 9. (Color online) Numerical check of the theoretical predictions of Eq. (21) for $y_f = 0$. In both panels the results of the simulations are divided by the theoretical value of $\text{MFPT}_{(0)}^{\circlearrowleft}$.

B. GMFPT

We define the GMFPT as the mean hitting time averaged on starting and on ending points:

$$\text{GMFPT} = \mathbb{E}_{i,f}[H(i,f)] = \frac{1}{V^2} \sum_{i \in \mathcal{V}} \sum_{f \in \mathcal{V}} H(i,f). \quad (24)$$

The GMFPT depends qualitatively on the topological properties of the underlying structure and this has been proven from different perspectives. For instance, it is well known that the GMFPT is related to the Kirchhoff index [50], $K = \mathbb{E}_{i,f}[R_{i,f}]$ [in fact, from Chandra's formula, $H(i,f) + H(f,i) = 2mR_{i,f}$ [51], it follows that $\text{GMFPT} = m\langle R \rangle$].
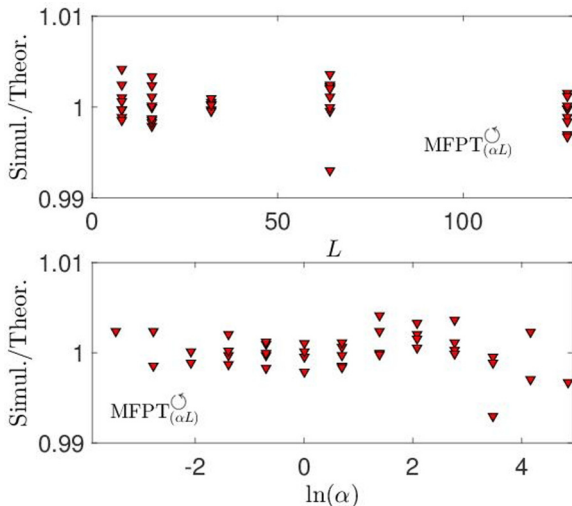

FIG. 10. (Color online) Numerical check of the theoretical predictions of Eq. (21) for $y_f = \alpha L$. In both panels the results of the simulations are divided by the theoretical value of $\text{MFPT}_{\alpha L}^{\circlearrowleft}$.

Moreover, a very general asymptotic expression was found in [52], reading as

$$\text{GMFPT}' \sim \begin{cases} V, & d_w < d_f, \\ V \ln(V), & d_w = d_f, \\ V^{d_w/d_f}, & d_w > d_f, \end{cases} \quad (25)$$

where d_w is the walk dimension and d_f is the fractal dimension. Their definition of the GMFPT is slightly different from ours: theirs is averaged over links,

$$\text{GMFPT}' = \frac{1}{m} \sum_{i,f \in \mathcal{V}} \frac{H(i,f)g(i)g(f)}{(m - g(f))},$$

while ours is averaged over vertices,

$$\text{GMFPT} = \frac{1}{V^2} \sum_{i,f \in \mathcal{V}} H(i,f).$$

Despite these different definitions they showed that these lead to the same asymptotics. Now, for the comb lattice the walk dimension d_w is not unique [53] and Einstein's relation $\tilde{d}\, d_w = 2d_f$ does not hold directly, hence one should calculate the GMFPT in a more "pedestrian" way. Now, we report the exact value of GMFPT for the comb structures outlined above and compare their asymptotic behaviors with Eq. (25).

1. Bidimensional open combs

To calculate the GMFPT for open combs, we start from Eq. (17). We recall that the MFPT_f can be written as the sum of two terms—the former depends on the final vertex, and the latter is $\text{MFPT}_{(0,0)}$—in a such way that in order to obtain the exact value of GMFPT we have to average only on the former; namely,

$$\text{GMFPT} = \mathbb{E}[f(x_f, y_f)] + \text{MFPT}_{(0,0)}. \quad (26)$$

After some algebra we find

$$\begin{aligned} \text{GMFPT} &= \sum_{x_f=-L}^{L} \sum_{y_f=-\alpha L}^{\alpha L} \text{MFPT}_f \quad (27) \\ &= \frac{1}{3(1+2L)(1+2L\alpha)}[8L^2(1+2\alpha+\alpha^2) \\ &\quad + 8L^3(1+8\alpha+8\alpha^2+\alpha^3) \\ &\quad + 8L^4(4\alpha+15\alpha^2+5\alpha^3) + 16L^5\alpha^2(2+3\alpha)], \end{aligned}$$

whose leading order is

$$\text{GMFPT}(L,\alpha) \sim L^3 \left(\frac{8}{3}\alpha + 4\alpha^2 \right). \quad (28)$$

We have numerically tested this result for many values of L and α, as shown in Fig. 11. In this figure we tuned L from 8 to 256 and α from 1/32 to 128.

2. Bidimensional closed combs

We now apply analogous arguments to calculate the exact value of the GMFPT for closed combs, hereafter referred to as the $\text{GMFPT}^{\circlearrowleft}$. Averaging $\text{MFPT}_f^{\circlearrowleft}$ over f, we find the exact
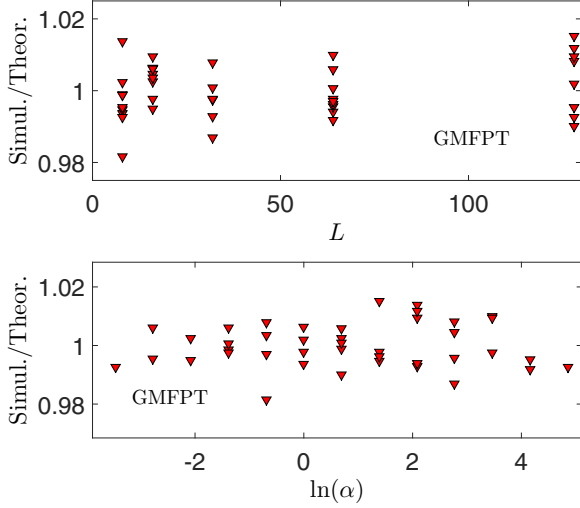
FIG. 11. (Color online) Numerical check of the theoretical predictions of Eq. (27). In both panels the results of the simulations are divided by the theoretical value of GMFPT.

value of $\text{GMFPT}^{\circlearrowleft}$ as

$$\text{GMFPT}^{\circlearrowleft}(L,\alpha) = \frac{2}{3}[L(1+2\alpha) + L^2(1+8\alpha+2\alpha^2) + L^3(2\alpha+6\alpha^2)], \tag{29}$$

whose leading order is

$$\text{GMFPT}^{\circlearrowleft}(L,\alpha) \sim L^3\left(\frac{4}{3}\alpha + 4\alpha^2\right). \tag{30}$$

We have numerically tested this result for many values of L and α, as shown in Fig. 12. In this figure we tuned L from 8 to 256 and α from 1/32 to 128.

Again, we note that the coefficient of α^2 is the same in both combs, but the coefficient of α^1 is not. For both GMFPT and $\text{GMFPT}^{\circlearrowleft}$ the leading order $\sim L^3$ is larger than the behavior expected from a more homogeneous structure with analogous
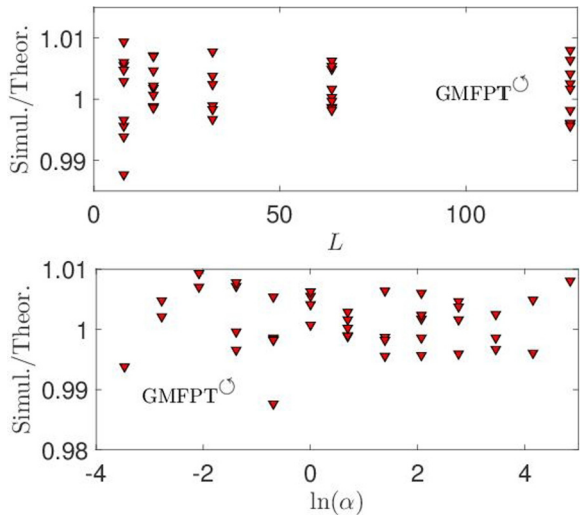

FIG. 12. (Color online) Numerical check of the theoretical predictions of Eq. (29). In both panels the results of the simulations are divided by the theoretical value of $\text{GMFPT}^{\circlearrowleft}$.

dimensions ($\tilde{d} = 3/2$ and $d_f = 2$). This highlights once more the peculiar behavior of combs.

IV. CHEMICAL-KINETICS PERSPECTIVE

In this section we frame the previous results within a chemical-kinetics perspective. Imagine having two reactants, say A (static) and B (dynamic). If we are allowed to choose the position of A, but we have no control of B (namely, we cannot fix its starting point), which will diffuse freely throughout the lattice, we can choose for the static reactant the place which minimizes the reaction time. In fact, this is just the node f that minimizes MFPT_f.

As shown in Secs. IIIA1 and IIIB2, the MFPT for both open and closed combs can be written as $\text{MFPT}_f = \phi(f) + \text{const}$, with $\phi(f) \geqslant 0$ for every final vertex f. In particular, in open combs the minimum value $\phi(f) = 0$ is recovered when $f = (0,0)$, and in closed ones when $f = (i,0)$. On the other hand, the maximum value of MFPT_f arises when the value of $\phi(f)$ is maximized; this occurs at $f = (\pm L, \pm \alpha L)$ for open combs and $f = (i, \pm \alpha L)$ for closed ones. Of course, for closed combs there is no dependence on the x coordinate due to the periodic condition on the x axis.

Now, if we cannot control the position of A, but this is stochastic, what is the typical time $\tau_f = \text{MFPT}_f$ it takes for the reaction to occur? In particular, the reaction is considered "slow" if $\tau_f > \text{GMFPT}$ and "fast" if $\tau_f < \text{GMFPT}$. We characterize the boundary between the two regimes finding those vertices f for which $\text{GMFPT} = \text{MFPT}_f$. We obtain these results in the limit $L \to \infty$ by imposing asymptotic equality between Eq. (20) and Eq. (28), and between Eq. (23) and Eq. (30). Recalling that $f = (x_f, y_f)$, we look for the functional form $y_f(x_f, L, \alpha)$ such that $\text{GMFPT} \sim \text{MFPT}_{\{x_f, y_f\}}$.

A. GMFPT vs MFPT_f in open combs

Let us consider the leading value of GMFPT and MFPT_f; from Eqs. (20) and (28),

$$\text{GMFPT}(L,\alpha) \sim L^3\left(\tfrac{8}{3}\alpha + 4\alpha^2\right),$$
$$\text{MFPT}_f(L,\alpha) \sim L^3\left\{4\alpha\left[\tfrac{1}{3} + X^2\right] + 8\alpha^2|Y|\right\},$$

where we have normalized the coordinates as $X = x_f/L$ and $Y = y_f/\alpha L$. Now the vertices f for which $\text{MFPT}_f = \text{GMFPT}$ are those whose coordinates fulfill the equality

$$\left(\frac{8}{3}\alpha + 4\alpha^2\right) = \left[4\alpha\left(\frac{1}{3} + X^2\right) + 8\alpha^2|Y|\right].$$

Solving for Y we find

$$|Y| = \left(\frac{1}{2} + \frac{1}{6\alpha}\right) - \frac{X^2}{2\alpha}.$$

One can see that the fraction of vertices for which the reaction is slow, F_{slow}, or fast, F_{fast}, is exactly the same for every value of α. In fact, $F_{\text{slow}} = \int_0^1 |Y(X,\alpha)|dX = \frac{1}{2}$. The phase diagram is shown in Fig. 13. As we can see, varying the value of α there are three possible scenarios: when α is sufficiently small there are some teeth totally composed of fast vertices (like for $\alpha = \frac{1}{3}$); when α is large enough there are no teeth that are completely fast or slow (like for $\alpha = \frac{2}{3}$ and $\alpha = 1$); and in the
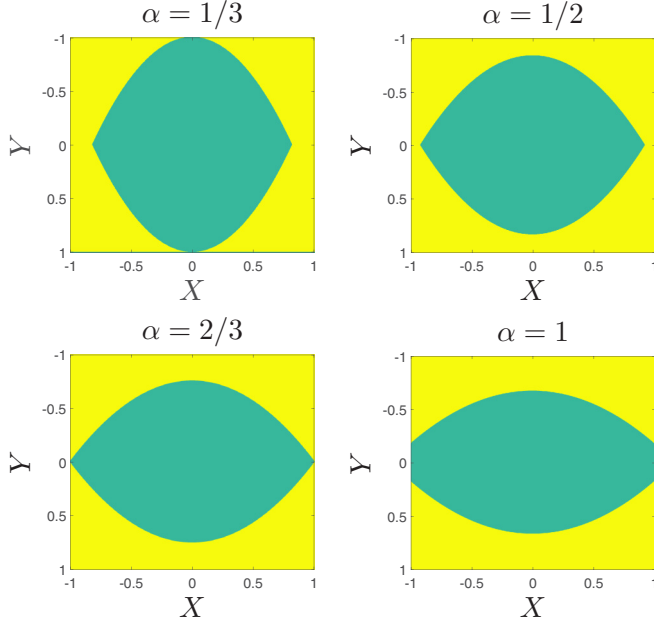
FIG. 13. (Color online) Phase diagram of $\mathrm{MFPT}_{\{X,Y\}} - \mathrm{GMFPT}$: vertices where $\mathrm{MFPT}_{\{X,Y\}} > \mathrm{GMFPT}$ are shown in yellow; those where $\mathrm{MFPT}_{\{X,Y\}} < \mathrm{GMFPT}$, in teal.

intermediate case there exist some teeth composed entirely of slow vertices but none composed completely of fast vertices (like for $\alpha = \frac{1}{2}$).

(a) The first case happens when $|Y| \geqslant 1$ for $X = 0$. This means that $|Y| = (\frac{1}{2} + \frac{1}{6\alpha}) \geqslant 1$, and solving for α, we find $\alpha \leqslant 1/3$.

(b) The second case occurs when $|Y| \geqslant 0$ for $X = 1$. This means that $|Y| = (\frac{1}{2} + \frac{1}{6\alpha}) - \frac{1}{2\alpha} \geqslant 0$, and solving for α, we find $\alpha \geqslant 2/3$.

(c) The last case happens in the intermediate case, $2/3 > \alpha > 1/3$.

B. GMFPT vs MFPT$_f$ in closed combs

Let us consider the leading terms of GMFPT and MFPT_f; from Eqs. (23) and (30)

$$\mathrm{GMFPT}^{\circlearrowleft} (L,\alpha) \sim L^3 \left(\frac{4}{3}\alpha + 4\alpha^2 \right),$$

$$\mathrm{MFPT}_f^{\circlearrowleft} (L,\alpha), \sim L^3 \left\{ \frac{4}{3}\alpha + 8\alpha^2 |Y| \right\},$$

and the set of vertices f for which $\mathrm{MFPT}_f \sim \mathrm{GMFPT}$ is those whose coordinates fulfill the equality

$$\left(\frac{4}{3}\alpha + 4\alpha^2 \right) = \left\{ \frac{4}{3}\alpha + 8\alpha^2 |Y| \right\}.$$

Solving for Y we find

$$|Y| = \frac{1}{2}.$$

This means that the location of nodes f such that $\mathrm{GMFPT} = \mathrm{MFPT}_f$ depends neither on X (and this is obvious due to the periodic boundary condition) nor on α. Therefore, if the target is placed sufficiently far from the backbone (i.e., at least at half the height of a tooth), the reaction turns out to be slow. Once again, the fraction of vertices giving rise to slow and fast reactions is the same. The phase diagram is shown in Fig. 14.
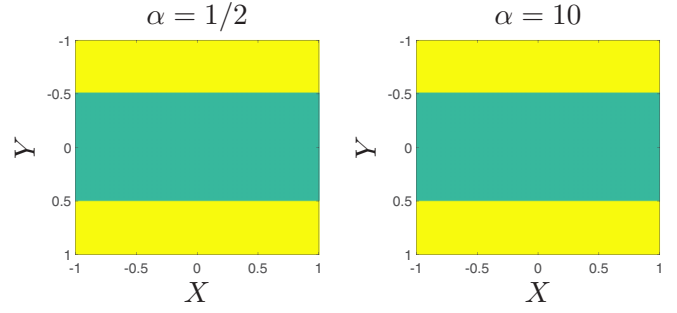

FIG. 14. (Color online) Phase diagram of $\mathrm{MFPT}^{\circlearrowleft}_{(Y)} - \mathrm{GMFPT}^{\circlearrowleft}$. Vertices where $\mathrm{MFPT}_{(Y)} > \mathrm{GMFPT}$ are shown in yellow; those where $\mathrm{MFPT}_{(Y)} < \mathrm{GMFPT}$, are in teal.

C. Inferring the position of the fixed reactant

Let us now consider a system where we can experimentally measure the MFPT to a given, fixed reactant A, whose position is not directly detectable. For instance, we can measure the absorbing time of a set of diffusing reactants initially placed randomly and in the presence of a fixed absorbing site. One can therefore exploit analytical formulas (17) and (21) in order to infer information about f from the experimental value of MFPT_f.

As for open combs, we recall that the leading behavior of MFPT_f is given by [see also Eq. (19)]

$$\mathrm{MFPT}_f = \phi + \mathrm{MFPT}_{0,0} \sim L^3 (4\alpha X^2 + 8\alpha^2 |Y|) + \frac{4\alpha L^3}{3},$$
(31)

where $X = x_f / L$ and $Y = y_f / \alpha L$ (as used in Sec. IV A). For any possible value of MFPT_f we can therefore detect a set of compatible positions of A, as envisaged in Fig. 15. More precisely, one can see that when $\alpha > 1/2$ (top), namely, when the linear size along the direction of side chains is relatively
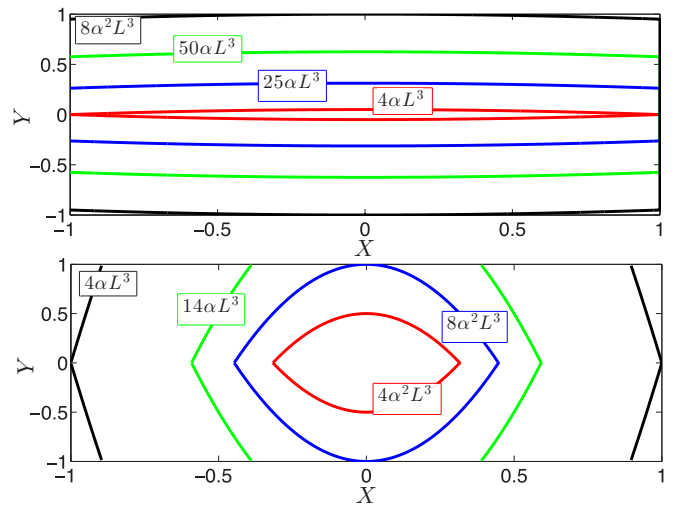

FIG. 15. (Color online) Each curve is associated with a different value of MFPT_f (as reported in the pertinent box) and represents the set of positions (X,Y) for A compatible with that value of the MFPT. Here we show results for $\alpha = 10$ (top) and for $\alpha = 1/10$ (bottom).

large, small values of MFPT_f always correspond to a reactant A placed close to the backbone; on the other hand, when $\alpha < 1/2$ (bottom), namely, when the linear size along the direction of the backbone is relatively large, small values of MFPT_f always correspond to a reactant A in the central side chains, although it can possibly be placed at peripheral sites. Otherwise stated, when $\alpha > 1/2$, the set of compatible positions, for a given (relatively small) value of MFPT_f, is flattened around the backbone; on the other hand, when $\alpha < 1/2$, the set of compatible positions, for a given (relatively small) value of MFPT_f, is flattened around the central tooth.

As for closed combs, this "inverse problem" is easier, as MFPT_f does not depend on the A projection along the backbone; in fact, recalling the leading term of MFPT_f [see also Eq. (22)],

$$\text{MFPT}_f^{\circlearrowleft} \sim L^3(8\alpha^2|Y|) + \frac{4\alpha L^3}{3}. \tag{32}$$

Therefore, for closed combs, the knowledge of MFPT_f yields no hint of the projection of A along the backbone, but its height can be derived univocally.

Finally, we mention that from experimental estimates for GMFPT, one we can infer the relation between L and α. This relation follows directly from (28) for open combs and from (30) for closed combs, and it reads as

$$L = \sqrt[3]{\frac{K\alpha + 4\alpha^2}{\text{GMFPT}}}, \tag{33}$$

where $K = 8/3$ for open combs, and $K = 4/3$ for closed ones.

V. CONCLUSIONS AND FUTURE PERSPECTIVES

In this work we have derived from Tetali's formula an alternative formula, (6), to calculate the exact value of the mean time $H(i, f)$ for a random walker first to reach a site f starting from a site i. This formula turns out to be particularly useful when the graph embedding the diffusion process is a branched structure. In particular, we have calculated explicitly the value of $H(i, f)$ for two-dimensional combs and its leading value for d-dimensional ones.

We have then used these results to calculate the MFPT_f and the GMFP for two-dimensional combs, highlighting that the leading value is composed of two terms: one proportional to αL^3 and the other one to $\alpha^2 L^3$, α being the ratio between the size of the backbone and the size of the teeth.

As for the GMFPT, we have noted that its asymptotic behavior does not directly depends on the comb fractal or spectral dimension (as for homogeneous lattices and fractals) and we have calculated it exactly.

Finally, we have discussed our results in the context of reaction kinetics. In fact, the MFPT can be seen as the mean time taken by a mobile reactant A to reach a static reactant B, when the starting point of the mobile reactant is not known. Interestingly, the typical time for the reaction to occur can be either larger (slow reaction) or smaller (fast reaction) than the GMFPT, and we have outlined the set of trap locations for which these regimes are recovered.

The results presented in this work could also be looked at as the starting point to approaching multiple-particle processes, where one considers a set of N diffusing particles, each reacting upon meeting any one of a group of M immobile fixed particles scattered throughout the comb lattice. Of course, these problems cannot be solved by simple generalizations of the solution of the $N = M = 1$ case, and specific techniques have to be developed [37,54].

[1] S. Havlin and D. Ben-Avraham, Adv. Phys. **36**, 695 (1987).

[2] I. M. Sokolov, Soft Matter **8**, 9043 (2012).

[3] R. Metzler and J. Klafter, Phys. Rep. **339**, 1 (2000).

[4] H. C. Berg, *Random Walks in Biology* (Princeton University Press, Princeton, NJ, 1993).

[5] T. Vicsek, *Fractal Growth Phenomena* (World Scientific, Singapore, 1989).

[6] G. Maret and P. E. Wolf, Z. Phys. B **65**, 409 (1987).

[7] E. F. Casassa and G. C. Berry, J. Polymer Sci. A **4**, 881 (1966).

[8] J. E. G. Lipson, D. S. Gaunt, M. K. Wilkinson, and S. G. Whittington, Macromolecules **20**, 186 (1987).

[9] A. Iomin and V. Méndez, Phys. Rev. E **88**, 012706 (2013).

[10] V. Méndez and A. Iomin, Chaos, Solitons Fractals **53**, 46 (2013).

[11] L. C. Y. Chu, D. Guha, and Y. M. M. Antar, IEEE Electron. Lett. **42**, 785 (2006).

[12] S. Havlin, J. E. Kiefer, and G. H. Weiss, Phys. Rev. A **36**, 1403 (1987).

[13] G. Weiss and S. Havlin, Philos. Mag. B **56**, 941 (1987).

[14] M. Thiriet, *Tissue Functioning and Remodeling in the Circulatory and Ventilatory Systems* (Springer, New York, 2013).

[15] M. A. Welte, Curr. Biol. **14**, R525 (2004).

[16] V. E. Arkhincheev, E. Kunnen, and M. R. Baklanov, J. Microelectr. **88**, 694 (2011).

[17] A. Iomin, Phys. Rev. E **73**, 061918 (2006).

[18] S. Burov, J.-H. Jeon, R. Metzler, and E. Barkai, Phys. Chem. Chem. Phys. **13**, 1800 (2011).

[19] A. Iomin, Phys. Rev. E **86**, 032101 (2012).

[20] K. H. Coats and B. D. Smith, Soc. Petrol. Eng. J. **4**, 73 (1964).

[21] E. Simanek, *Inhomogeneous Superconductors: Granular and Quantum Effects* (Oxford University Press, Oxford, UK, 1994).

[22] B. Kahng and S. Redner, J. Phys. A **22**, 887 (1989).

[23] D. Bertacchi, N. Lanchier, and F. Zucca, Ann. Appl. Prob. **21**, 1215 (2011).

[24] M. Krishnapur and Y. Peres, Elect. Comm. in Probab. **9**, 72 (2004).

[25] R. Campari and D. Cassi, Phys. Rev. E **86**, 021110 (2012).

[26] E. Agliari, A. Blumen, and D. Cassi, Phys. Rev. E **89**, 052147 (2014).

[27] P. Veng-Pedersen, Clin. Pharmacokin. **17**, 345 (1989).

[28] A. Szabo, K. Schulten, and Z. Schulten, J. Chem. Phys. **72**, 4350 (1980).

[29] E. W. Montroll, J. of Math. Phys. **10**, 753 (1969)

[30] A. Blumen, A. Volta, A. Jurjiu, and T. Koslowski, J. Lumin. **111**, 327 (2005).

[31] P. Fauchald and T. Tveraa, Ecology **84**, 282 (2003).

[32] A. L. Lloyd and R. May, Science **292**, 1316 (2001).

[33] S. Condamin, O. Benichou, V. Tejedor, R. Voituriez, and J. Klafter, Nature (London) **450**, 77 (2007).

[34] S. Condamin, O. Bénichou, and M. Moreau, Phys. Rev. Lett. **95**, 260601 (2005).

[35] B. Meyer, E. Agliari, O. Benichou, and R. Voituriez, Phys. Rev. E **85**, 026113 (2012).

[36] E. Agliari, Phys. Rev. E **77**, 011128 (2008).

[37] S. Redner, *A Guide to First-Passage Processes* (Cambridge University Press, Cambridge, UK, 2001).

[38] R. Metzler, G. Oshanin, and S. Redner, *First-Passage Phenomena and Their Applications* (World Scientific, Singapore, 2014).

[39] E. Agliari, R. Burioni, D. Cassi, and F. M. Neri, Theor. Chem. Acc. **118**, 855 (2007).

[40] N. Agmon, Chem. Phys. Lett. **497**, 184 (2010).

[41] A. Rebenshtok and E. Barkai, Phys. Rev. E **88**, 052126 (2013).

[42] S. Condamin, V. Tejedor, R. Voituriez, O. Bénichou, and J. Klafter, Proc. Natl. Acad. Soc. USA **105**, 5675 (2008).

[43] P. G. Doyle and J. L. Snell, *Random Walks and Electric Networks* (Mathematical Association of America, Oberlin, OH, 1994).

[44] P. Tetali, J. Theor. Prob. **4**, 101 (1991).

[45] S. C. Chang and L. C. Chen, arXiv:0806.0701.

[46] R. Burioni, D. Cassi, and F. M. Neri, J. Phys. A **37**, 8823 (2004).

[47] O. Matan and S. Havlin, Phys. Rev. A **40**, 6573 (1989).

[48] J. J. Kozak and V. Balakrishnan, Phys. Rev. E **65**, 021105 (2002).

[49] A. Baronchelli and V. Loreto, Phys. Rev. E **73**, 026103 (2006).

[50] D. J. Klein, J. Douglas, and M. Randić, J. Math. Chem. **12**, 81 (1993).

[51] A. K. Chandra, P. Raghavan, W. L. Ruzzo, R. Smolenksy, and P. Tiwari, Comput. Complex. **6**, 312 (1996).

[52] V. Tejedor, O. Bénichou, and R. Voituriez, Phys. Rev. E **80**, 065104 (2009).

[53] D. Bertacchi and F. Zucca, J. Austral. Math. Soc. **75**, 325 (2003).

[54] L. Acedo and S. B. Yuste, Recent Res. Devel. Stat. Phys. **2**, 83 (2002).